Remote Sensing of Environment 166 (2015) 106–115

Contents lists available at ScienceDirect

Remote Sensing of Environment

journal homepage: www.elsevier.com/locate/rse

Suomi NPP VIIRS reflective solar band on-orbit radiometric stability and accuracy assessment using desert and Antarctica Dome C sites

Sirish Uprety [a,*], Changyong Cao [b]

[a] Cooperative Institute for Research in the Atmosphere (CIRA), Colorado State University, Fort Collins, CO, 80523, USA
[b] Center for Satellite Applications and Research NOAA/NESDIS, College Park, MD, 20740, USA

ARTICLE INFO

Article history:
Received 18 December 2014
Received in revised form 4 May 2015
Accepted 23 May 2015
Available online 16 June 2015

Keywords:
VIIRS
MODIS
OLI
Calibration
Intercomparison
Radiometric stability
Radiometric accuracy
Dome C
Libya 4
Bias

ABSTRACT

The Visible Infrared Imaging Radiometer Suite (VIIRS) is a key instrument flying aboard Suomi NPP satellite. It is a follow on mission for NOAA series AVHRR and NASA MODIS. The radiometric stability and accuracy of VIIRS are critical to make its data useful for weather and climate applications. This study is focused on analyzing VIIRS radiometric performance using well established calibration sites and through the inter-comparison with other satellite instruments such as AQUA MODIS and Landsat 8 OLI. The paper analyzes stability of VIIRS reflective solar bands over more than two years by using sites such as Libya 4, Sudan 1 and Dome C. VIIRS absolute radiometric accuracy is quantified using AQUA MODIS over the above mentioned sites. For VIIRS band M11 (2.1 μm), since there is no matching MODIS band pair, this study uses matching SWIR band from Landsat 8 OLI as a reference to quantify the absolute calibration accuracy of M11. The study shows that VIIRS moderate resolution reflective solar bands are stable with better than 0.5% for most of the bands with uncertainty on the order of 1%. After accounting the spectral differences, the absolute radiometric bias estimated through VIIRS and MODIS inter-calibration is within 2% for bands M1–5 and M10 and about 3% for bands M7–8. Similarly, M11 bias estimated using VIIRS and OLI inter-comparison is 5.4%.

1. Introduction

Visible Infrared Imaging Radiometer Suite (VIIRS) is a key NOAA satellite instrument onboard S-NPP satellite that provides data for the ocean, land, aerosol, and cloud applications. VIIRS instrument is equipped with onboard calibration (OBC) system that consists of solar diffuser with stability monitor for tracking the performance of Reflective Solar Bands (RSB) and blackbody for Thermal Emissive Bands (TEB). More detailed information on VIIRS instrument characteristics has been summarized by Cao, Deluccia, et al., 2013. The satellite data quality needs to be validated independently to ensure the stability and accuracy of OBC and to ensure that the satellite data from different instruments on different satellite platforms have a common radiometric scale. On-orbit radiometric stability and accuracy can be evaluated independently using different techniques such as trending and inter-calibration using vicarious calibration sites, SNO and SNO-x based inter-comparison, lunar trending, Deep Convective Clouds (DCC), etc. (Cao, Xiong, et al., 2013; Chander, Mishra, et al., 2010; Chander, Xiong, Choi, & Angal, 2010; Helder et al., 2013; Markham et al., 2014; Uprety et al., 2013; Wu, 2004; Xiong et al., 2008).

Several studies in the past have discussed different aspects of the on-orbit calibration and validation of VIIRS using independent techniques (Bhatt et al., 2014; Cao, Xiong, et al., 2013; Uprety et al., 2013; Wang & Cao, 2014; Wu, Sullivan, & Heidinger, 2011). Previous study by Uprety et al. (2013) presents the VIIRS radiometric accuracy by intercomparing with MODIS using extended simultaneous nadir overpass (SNO-x) over desert and ocean. The technique was inherited from SNO based intercomparison and it was an early assessment on VIIRS on-orbit performance using less than a year of VIIRS observation. Only VIIRS bands M1 to M8 were analyzed. Similarly, Wu, Cao, and Sun (2013) discuss VIIRS and MODIS intercomparison using high latitude polar SNOs and desert site for moderate resolution bands M1–7. Earlier study by Wang & Cao (2014) discusses VIIRS on-orbit radiometric stability for bands M5 and M7 by trending the mode of Deep Convective Cloud (DCC) pixels. Similarly the earlier study by Bhatt et al. (2014) presents the results on early assessment of VIIRS radiometric stability using Libya-4 site and DCC. Bands I1, I3 and M1–11 except M2–3 and M8 were analyzed using the VIIRS observations from early 2012 till the late 2013.

This paper presents the comprehensive study and analysis on VIIRS radiometric performance for bands M1 (0.4 μm) through M11 (2.1 μm) (except bands M6 and M9 (1.37 μm)) characterized using the two Saharan desert calibration sites, Libya-4 and Sudan-1 and Antarctica Dome C site. In addition, inter-comparison of VIIRS with

* Corresponding author.
E-mail addresses: sirish.uprety@noaa.gov (S. Uprety), changyong.cao@noaa.gov (C. Cao).

http://dx.doi.org/10.1016/j.rse.2015.05.021
0034-4257/

AQUA MODIS and Landsat 8 Operational Land Imager (OLI) is performed to quantify the radiometric accuracy of VIIRS. Both Libya-4 and Dome C are CEOS endorsed calibration sites. The temporal trends of TOA reflectance observed at nadir are used to quantify the radiometric stability. VIIRS radiometric accuracy can be achieved by continuously monitoring, characterizing and comparing VIIRS instrument to other well calibrated radiometers such as MODIS whose absolute calibration uncertainty is estimated to be within 2% (Xiong et al., 2007). This paper shows absolute radiometric bias of VIIRS estimated for moderate resolution radiometric bands by comparing top of atmosphere (TOA) reflectance with MODIS and OLI. The spectral coverage of one of the VIIRS moderate resolution bands M11 (2.2 μm) doesn't overlap with MODIS. Hence we have used Landsat 8 OLI SWIR band 2 (2.11–2.29 μm), a new generation Landsat sensor, to perform the intercomparison over Libya-4 and evaluate the radiometric accuracy. VIIRS M11 signal strength over desert (~7–8 W/m^2-sr-um) is more than 10 times higher than over ocean. Typical radiance observed by M11 over ocean is less than 0.5 W/m^2-sr-um. This very small signal strength over ocean can significantly increase the noise level in measurements and makes the band more challenging for calibration in absolute scale. Assuming that the detector gain is linear, we have chosen desert sites to study its radiometric performance. In addition, we have used OLI to evaluate the radiometric performance of VIIRS M7. This helps to compare the results from VIIRS, MODIS intercomparison for band M7 and analyze any discrepancy and its root cause. The uncertainties in the VIIRS bias are mainly due to the spectral difference between the instruments matching bands, BRDF, cloud contamination, calibration issues, and registration errors. Uncertainty in bias caused by mismatch in relative spectral response (RSR) of the instruments is quantified using EO-1 Hyperion and radiative transfer models such as MODTRAN (Uprety et al., 2013). After accounting spectral differences, the residual bias observed at different sites is compared and analyzed. Unlike the previous studies that analyzed the VIIRS stability for only few bands, this study analyzes more VIIRS bands that include all SWIR bands except M9 and for a longer time interval ranging from early 2012 to the end of 2014. Further, in addition to Libya-4, it utilizes Sudan-1 and Dome C sites to supplement and validate the radiometric stability and accuracy results. Also, besides Aqua MODIS, it uses OLI to compare VIIRS M7 and M11 thus providing further opportunities to better understand and improve the calibration accuracy of these bands. This comprehensive analysis on VIIRS radiometric performance helps to build the confidence to users working on EDR products.

2. Methodology

There exist Earth locations which are temporally stable and are capable of tracking the changes in satellite instrument response over time. These are usually high altitude arid regions with little rainfall, mostly clear sky with no human activities. Since it is almost impossible to find a single site with all above ideal characteristics, the term Pseudo Invariant Calibration Sites (PICS) has been commonly used for these sites which have been identified and characterized to be suitable to detect the radiometric stability of satellite sensors. More details on PICS and its optimized identification criteria can be found in earlier studies such as Helder, Basnet, and Morstad (2010). Saharan desert calibration sites have been used in trending the satellite sensors for more than a decade (Helder et al., 2008, 2010, 2013; Markham et al., 2004, 2012; Barsi, Markham, Helder, & Chander, 2007; Rao & Chen, 1995, 1999; Wu, 2004, Wu, Sullivan, & Heidinger, 2011). In addition, the potential of these sites for absolute calibration has been successfully demonstrated by several studies in the past (Helder et al., 2013; Mishra, Haque, et al., 2014; Mishra, Helder, Angal, Choi, & Xiong, 2014). PICS can be used reliably to analyze radiometric performance of the instruments as long as the sites have been rigorously characterized to ensure the long term stability.

2.1. Calibration sites

This study uses Saharan desert sites and Antarctica Dome C (75.1°S, 123.39°E) site. The desert sites used are Libya-4 (28.55°N, 23.39°E) and Sudan-1 (21.74°N, 28.22°E). Libya-4 is one of the Committee on Earth Observation Satellites (CEOS) endorsed calibration sites and has been widely used in calibration and validation of medium and high resolution satellites (Chander, Mishra, et al., 2010; Chander, Xiong, et al., 2010; Cosnefroy, Leroy, & Briottet, 2014; Helder et al., 2010; Helder et al., 2013, Markham and Helder, 2012; Wu, Xiong, Cao, & Angal, 2008). Libya-4 is one of the best desert reference sites recommended by CEOS. More detailed analysis on the radiometric quality of Saharan desert sites can be found in Helder et al. (2010) and Teillet, Barsi, Chander, and Thome (2007), Teillet, Fedosejevs, Thome, and Barker (2007). Fig. 1 shows VIIRS image with Libya-4 and Sudan-1 sites. The reason behind choosing Sudan 1 site is that NOAA series AVHRR sensors use this site for on-orbit relative calibration (Wu, 2004). In recent years some of the areas near the Sudan-1 site started to suffer from human activities that include irrigation (Yu & Wu, 2009) however, the region of interest chosen for this study avoided the areas impacted by human activities.

Antarctica Dome C (−75.1°, 123.39°) is a large snow flat surface located at an altitude of 3.2 km from sea level. It is a CEOS endorsed calibration site. The site has excellent temporal stability and spatial uniformity (Cao et al., 2010; Uprety & Cao, 2011, 2012). It has been studied rigorously due to its unique characteristics such as, high altitude; high reflectance; high percentage of cloud-free time; atmosphere with very low infrared sky emission, low water vapor content and low aerosol and dust content. Some of the limitations of this site include: it receives sunlight only for about four months every year (austral summer only), there is a large BRDF from snow, accessibility issues for ground truth measurements, early launch cal/val activities may not be possible for RSB if the satellite is launched during the other 8 month period. The site is observed more frequently by polar orbiting satellites however it is not visible for current GOES and future GOES-R instruments.

2.2. Sensor overview

S-NPP is a sun-synchronous polar orbiting satellite launched in October 2011 with VIIRS as one of the payloads. VIIRS has full global coverage of Earth daily (one at daytime and the other at nighttime) from a nominal altitude of 829 km. It is a multispectral scanning radiometer with 16 moderate resolution bands (0.4 μm to 12 μm), 5 Imagery bands (0.6 μm to 12 μm) and 1 day night band (DNB). This is a wide-swath (3000 km) scanning radiometer with spatial resolution: 750 m for moderate resolution bands and DNB, 375 m for imagery bands. It is a follow-on mission for Advanced Very High Resolution Radiometer (AVHRR) on NOAA and MetOp series satellites and Moderate-Resolution Imaging Spectroradiometer (MODIS) onboard Terra and Aqua. More detailed explanation on VIIRS instrument and onboard calibrators can be found in Cao, Deluccia, et al. (2013).

MODIS is a NASA instrument launched aboard Terra (1999) and Aqua (2002) satellites. It has 36 spectral bands with wavelengths ranging from 0.4 to 14.4 μm. The spatial resolution varies from 0.25 km for the first two bands, 0.5 km for 5 bands and 1 km for the remaining 29 bands. A complete scan covers a swath width of 10 km (along track) and 2330 km (cross track) with +/− 55° scan angle. Absolute radiometric calibration for both VIIRS and MODIS is achieved by using onboard calibration system that mainly includes solar diffuser and solar diffuser stability monitor for the calibration of reflective solar bands (RSBs) and blackbody for the thermal emissive bands. More detailed explanation on MODIS instrument can be found in Xiong and Barnes (2006).

The Operational Land Imager (OLI) is a pushbroom sensor launched onboard Landsat 8 on 11 February 2013. Detail explanations on the instrument design including onboard calibration, characterization and performance can be found in earlier studies such as Irons, Dwyer, and

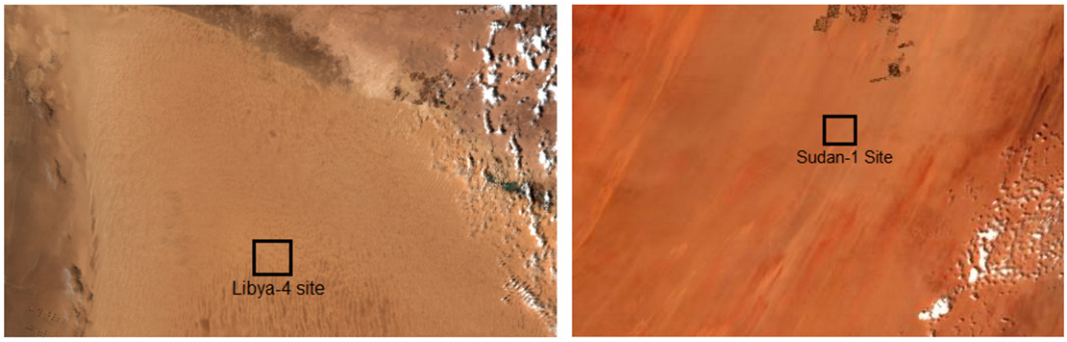

Fig. 1. Libya-4 and Sudan-1 sites are shown in VIIRS color image.

Barsi (2012), Knight and Kvaran (2014), Markham et al. (2012, 2014). OLI collects images using nine spectral bands with spatial resolution ranging from 30 m (bands 1–7, 9) and 15 m for panchromatic band. It covers a swath width of 183 km. RSB calibration is performed through onboard calibration which consists of two solar diffusers and three pairs of lamps. One solar diffuser panel is exposed to sunlight regularly whereas the other diffuser panel is exposed infrequently. The former solar panel is used to detect changes in the working panel spectral reflectance due to frequent solar exposure. Irons et al. (2012) have explained in detail about the OLI instrument design and onboard calibration system.

The EO-1 Hyperion is a push broom hyperspectral sensor launched by NASA on November 21, 2000. It images the earth in 220 spectral bands (http://eo1.usgs.gov/sensors/hyperion) with wavelengths ranging from 0.4 μm to 2.5 μm. Hyperion has a footprint size of 30 m and the swath width of 7.5 km. The radiometric stability of the instrument is maintained using solar, lunar and onboard calibration sources (Folkman, Pearlman, Liao, & Jarecke, 2001; Pearlman et al., 2003).

2.3. Instrument relative spectral response functions

Relative spectral response functions of VIIRS bands under study are shown in Fig. 2. In addition, the figure also shows matching VIIRS bands with MODIS and OLI. Fig. 2 indicates that VIIRS SWIR band M11 (2.2 um) doesn't overlap with MODIS. OLI SWIR band 2 (2.2 um) has wider spectra but its bandwidth completely covers the VIIRS M11 RSR. VIIRS M7 band is compared with both MODIS and OLI over desert sites to evaluate their radiometric consistency. In general, VIIRS bands are much narrower than MODIS and OLI. This small difference in spectral coverage for matching bands results in slightly different at-sensor radiance/reflectance even when both the sensors are observing the same target. This is one of the reasons that it is always desirable to

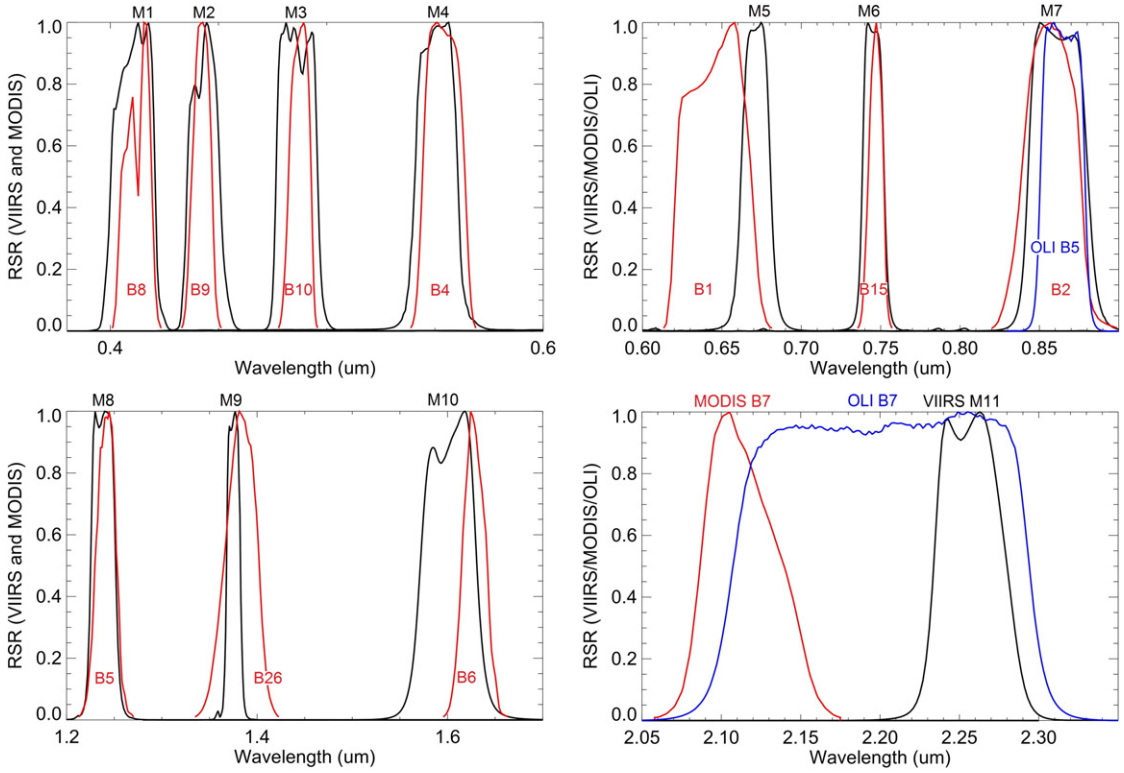

Fig. 2. Instrument RSRs showing VIIRS (black) matching bands with MODIS (red) and OLI (Blue). Bottom right shows VIIRS M11 (2.2 μm) RSR that is completely covered by OLI but not by MODIS.

perform the comparison over calibration sites which are either spectrally flat or are rigorously characterized in spectral domain.

2.4. Data processing

For VIIRS data used in this study, the Interface Data Processing Segment (IDPS) generated scientific data record (SDR) for 9 moderate resolution RSB (except M6 (0.74 μm) and M9 (1.375 μm cirrus band)) is downloaded from NOAA CLASS (www.class.ngdc.noaa.gov). Spatial resolution of data is 0.742 km at nadir. For MODIS, 1 km L1b data were used (http://ladsweb.nascom.nasa.gov/data/). MODIS data used are collection 6 version. For Landsat 8 OLI, level 1 terrain corrected geotiff data with resolution of 30 m are downloaded from USGS (http://earthexplorer.usgs.gov/).

VIIRS and MODIS nadir overpass data over the calibration sites are collected from May 2012 till November 2014. There was a major VIIRS SDSM transmission screen update during early 2012 which caused large change in VIIRS response during March/April 2012. Hence this study analyzes VIIRS starting from early May 2012 considering VIIRS calibration to be more stable then after. Radiometric performance is analyzed in two key aspects which are radiometric stability and absolute radiometric accuracy. Radiometric stability is evaluated using temporal trends at sensor TOA reflectance and radiometric accuracy is analyzed by comparing VIIRS measurements with MODIS and OLI.

The following steps summarize how data processing is performed for each band.

a) For each nadir overpass of the satellite, a region of interest (ROI) of size 30 km × 30 km is extracted such that the center of ROI has same latitude and longitude as defined for each site in earlier section.
b) Each ROI needs to be checked for a number of filtering criteria. Only the ROI with all clear sky pixels is considered for analysis. Cloud mask product from VIIRS and MODIS is used to determine the level of cloud contamination.
c) A spatial uniformity test is also performed such that the given ROI is considered valid only if its spatial uniformity (ratio of 1 standard deviation to mean reflectance) is better than 4%. This helps to filter out most of the cloud contaminated data.
d) In addition, a threshold of $\pm 6^0$ sensor zenith for all pixels within an ROI is used to limit the analysis only within nadir.

After an ROI passes all above conditions, mean and standard deviation are calculated and a temporal trend is generated for each instrument. All data analysis is performed using at-sensor TOA reflectance. TOA reflectance of VIIRS can be read directly from SDR data product. However, the data are stored as scaled TOA reflectance. Scaling factors are available for each band to convert the data to reflectance. MODIS and OLI give TOA reflectance before accounting for solar zenith angle.

Small differences in spectral shape and coverage of matching bands between two instruments result in bias even when both the instruments observes the same target at the same time. This bias needs to be accounted for during the inter-comparison. This is commonly termed as spectral band adjustment factor (SBAF). When two instruments are compared after applying SBAF correction, the residual bias trend shows the radiometric consistency over time. Spectrally induced bias can be calculated by taking the ratio of VIIRS equivalent reflectance and MODIS or OLI equivalent reflectance obtained by convolving Hyperion reflectance spectra with instrument RSR (Uprety and Cao, 2012; Uprety et al., 2013).

3. Results and discussion

Section 3.1 explains the radiometric stability of VIIRS characterized using at sensor TOA reflectance trends. Sections 3.2 through 3.4 analyze the radiometric accuracy of VIIRS estimated through sensor inter-comparison. OLI is used to supplement the comparison results for bands M7 (0.86 μm) and M11 (2.2 μm). VIIRS band M6 (0.74 um) is not analyzed since the detectors get saturated over desert and snow. VIIRS, MODIS and OLI observe calibration sites at slightly different local time and few days apart. Hence the reflectance time series cannot be compared directly to estimate the bias before being accounted for BRDF. Since the BRDF at nadir over desert is dominated by solar zenith angles, the instruments are compared at similar solar zenith angles.

3.1. Radiometric stability of VIIRS

Time series of VIIRS and MODIS TOA reflectance since early May 2012 for bands M1, M4–8, M10 and M11 over Libya 4 and Sudan 1 are shown in Fig. 3. M2–3 behave similar to M1 and hence are not shown in the figure. VIIRS suggests larger short term (within few weeks) variability although the temporal trends are more stable. In addition, time series suggest that VIIRS agreement with MODIS is not consistent, indicating the change in VIIRS stability and accuracy over time. One such example is a major H-factor update that occurred at the end of May 2014 which led to sudden increase in VIIRS bands (such as M1 and M2) by approximately 2%. This can have larger impacts in the EDR products such as ocean color that has stringent requirements in calibration. One of the reasons for short term changes in VIIRS stability and accuracy is due to the calibration updates and anomalies that usually happen for short time intervals and is not usually noticeable due to larger variability and sparse time series.

Radiometric stability is analyzed by normalizing the reflectance time series by a BRDF function and doing a linear fit. BRDF is generated using a quadratic function of reflectance versus solar zenith angle assuming that impact due to relative azimuth and sensor zenith are insignificant (Uprety and Cao, 2012) at nadir observation. A statistical null hypothesis test was performed on the significance of slope i.e. slope = 0 at alpha = 0.05 for all bands. It was observed that most of the bands rejected the hypothesis test, indicating no significance of slope. Table 1 shows the radiometric stability of VIIRS in terms of temporal change (degradation) over nearly two and half years along with the uncertainty of 1-sigma standard deviation. Temporal degradation values are provided for bands with statistically significant slopes.

Fig. 3 indicates that M7 is the least stable band with calibration stability 1.5%. M11 temporal trend is stable however it is the noisiest band with variability (1-sigma standard deviation) greater than 1.5%. The TOA reflectance is calculated assuming the target characteristics to have Lambertian behavior even though the desert surface is not a true Lambertian target. In addition, most of the Earth view signal received by the sensor for visible bands (especially blue bands) comes from atmosphere. Thus the at-sensor reflectance is less dominated by the strong BRDF of surface. For nadir observations used in this study, the BRDF is mainly due to the annual variation of solar zenith angle. This is one of the reasons that annual oscillation is not easily noticed for bands such as M1–4. As the wavelength increases, i.e. for NIR and SWIR bands, the signal strength is mostly dominated by ground surface reflectance rather than from atmosphere. Thus the at-sensor TOA reflectance suggests good correlation with seasonal variation. Strong and well defined seasonal oscillation can be observed mainly for bands M7–11 shown in Fig. 3.

Fig. 4 shows VIIRS reflectance time series over Dome C. Bands M2 and M3 are not shown since their matching MODIS bands are mostly saturated over snow and very few data exists at higher solar zenith angles greater than 70°. For bands M5 and M7, the Dome C data from early October to late December are excluded in generating the BRDF function and stability analysis. This is mainly due to the hysteresis nature of Antarctica snow albedo i.e. the albedo in the morning and the afternoon is not the same for identical solar zenith angles (McGuffie and Henderson-Sellers, 1985; Yamanouchi, 1983). Figure shows large BRDF of more than 10% annually, indicated by the maximum variation in Dome C reflectance due to the annual variation in solar zenith angle. Majority of the bands

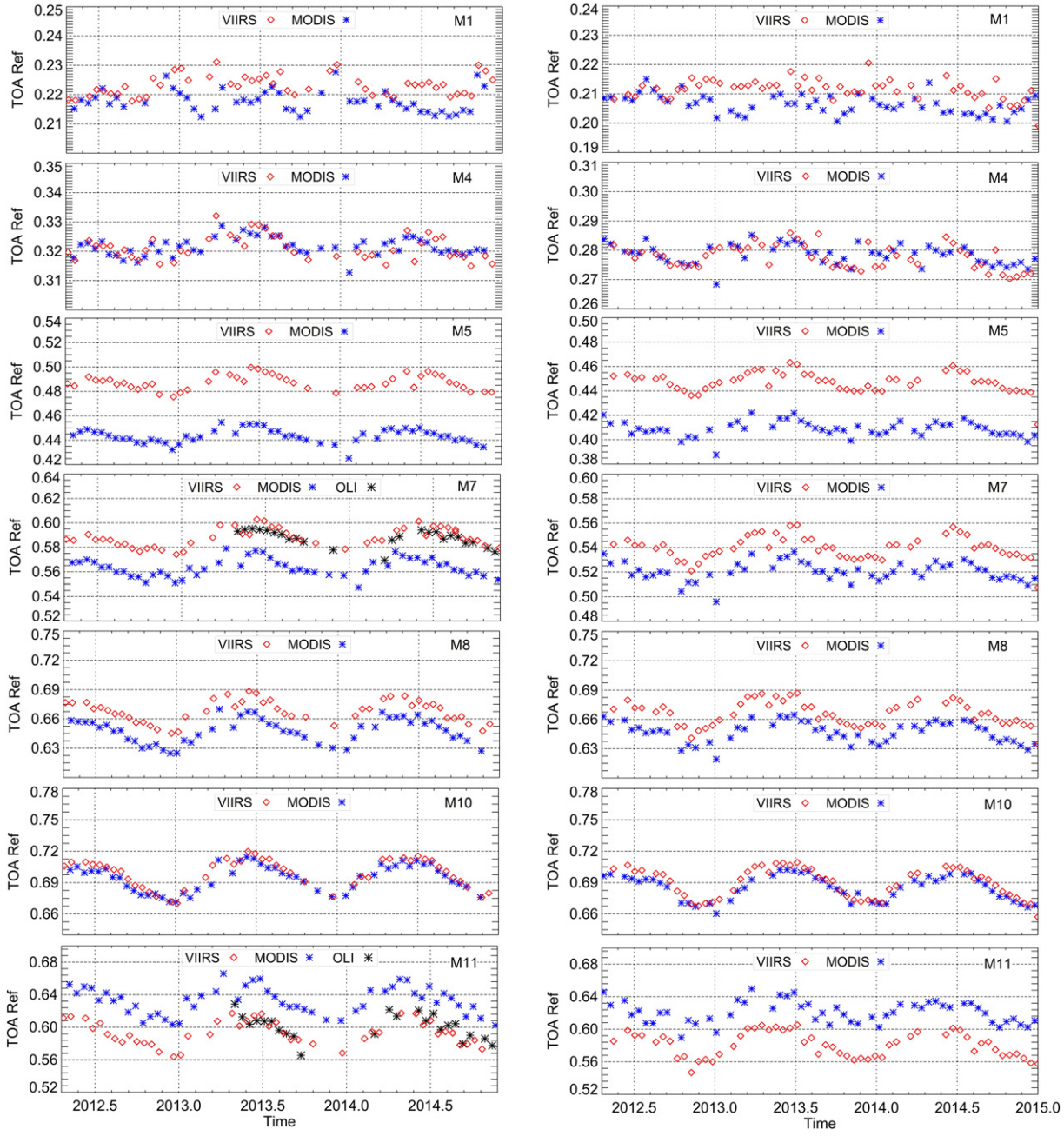

Fig. 3. VIIRS and MODIS TOA reflectance over left: Libya-4 and right: Sudan-1 sites along with OLI reflectance over Libya 4 for NIR (0.86 μm) and SWIR (2.2 μm) bands.

Table 1
Calibration stability of VIIRS RSB over calibration sites. Stability is calculated as a percent change over the period of analysis using linear trends fitted over BRDF normalized VIIRS time series.

VIIRS		MODIS		Radiometric stability		
Band	Wavelength (μm)	Band	Wavelength (μm)	Libya 4	Sudan 1	Dome C
M1	0.402–0.422	8	0.405–0.420	0.00% ± 1.20%	0.00% ± 1.23%	0.00% ± 0.60%
M2	0.436–0.454	9	0.438–0.448	0.00% ± 0.93%	0.00% ± 1.29%	0.94% ± 0.55%
M3	0.478–0.498	10	0.483–0.493	0.00% ± 0.98%	0.00% ± 1.31%	0.69% ± 0.51%
M4	0.545–0.565	4	0.545–0.565	0.00% ± 1.14%	0.00% ± 1.14%	0.00% ± 1.27%
M5	0.662–0.682	1	0.620–0.670	0.00% ± 0.79%	0.00% ± 0.94%	0.00% ± 0.96%
M7	0.846–0.885	2	0.841–0.876	1.50% ± 0.75%	1.45% ± 1.00%	0.00% ± 0.84%
M8	1.230–1.250	5	1.230–1.250	0.67% ± 0.91%	1.28% ± 1.07%	–
M10	1.580–1.640	6	1.628–1.652	0.78% ± 0.49%	0.70% ± 0.53%	–
M11	2.225–2.275	7	2.105–2.155	0.00% ± 1.60%	0.00% ± 1.49%	–

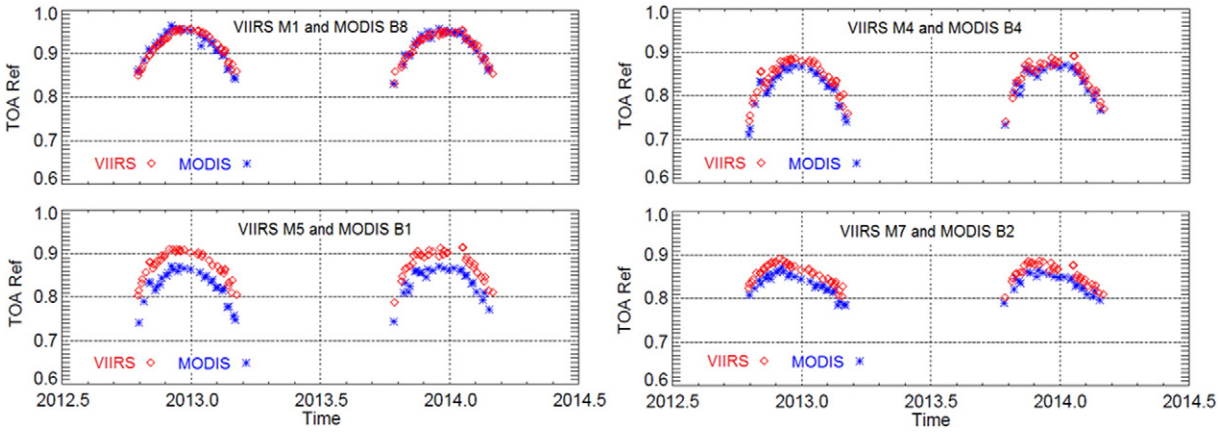

Fig. 4. VIIRS and MODIS reflectance time series over Dome C.

suggest no significant slopes with M1 being the most stable (Table 1) with 0.6% variability.

3.2. VIIRS intercomparison with MODIS and OLI

VIIRS radiometric accuracy is quantified by extracting the bias trends as a function of solar zenith angles (Fig. 5). This reduces the impact of uncertainty due to seasonal variation. Figs. 5a and 4b indicate that the VIIRS blue (M1–3) and green (M4) bands agree better with MODIS to within 2% as compared to red (M5), NIR (m7) and SWIR (M8–M11) bands. MODIS band 10 (matching VIIRS M3) gets saturated at high solar elevation and thus the VIIRS bias trend starts from nearly 35° solar zenith angle. VIIRS M4 (0.55 μm) indicates the smallest bias of less than 0.25% whereas M5 (0.64 μm) indicates the largest bias of more than 9.5% over Libya-4 and 10.05% over Sudan-1 sites. Earlier study by Uprety et al., 2013 have shown that the large bias in VIIRS M5 can be explained mainly due to RSR differences. A more detailed analysis on RSR differences is covered in section 3.3.1. The uncertainty which is provided as 1-sigma standard deviation is less than 1% for all bands except the SWIR bands. Impact on bias due to calibration updates and anomalies which usually happen for short time intervals is generally not noticeable. This is mainly due to sparse data (16 days apart) sets and the uncertainty on the order of 1%.

Fig. 5c shows the VIIRS bias trends relative to MODIS estimated over Dome C. It suggests larger rate of change in bias as a function of solar zenith angle compared to desert sites. Similarly, VIIRS M7 and M11 radiometric accuracy is also analyzed using Landsat 8 OLI SWIR band 2 (2.2 um). This is mainly because OLI SWIR band 2 fully covers the VIIRS band M11. One of the major improvements with Landsat 8 OLI compared to previous generation Landsat instruments is that there is

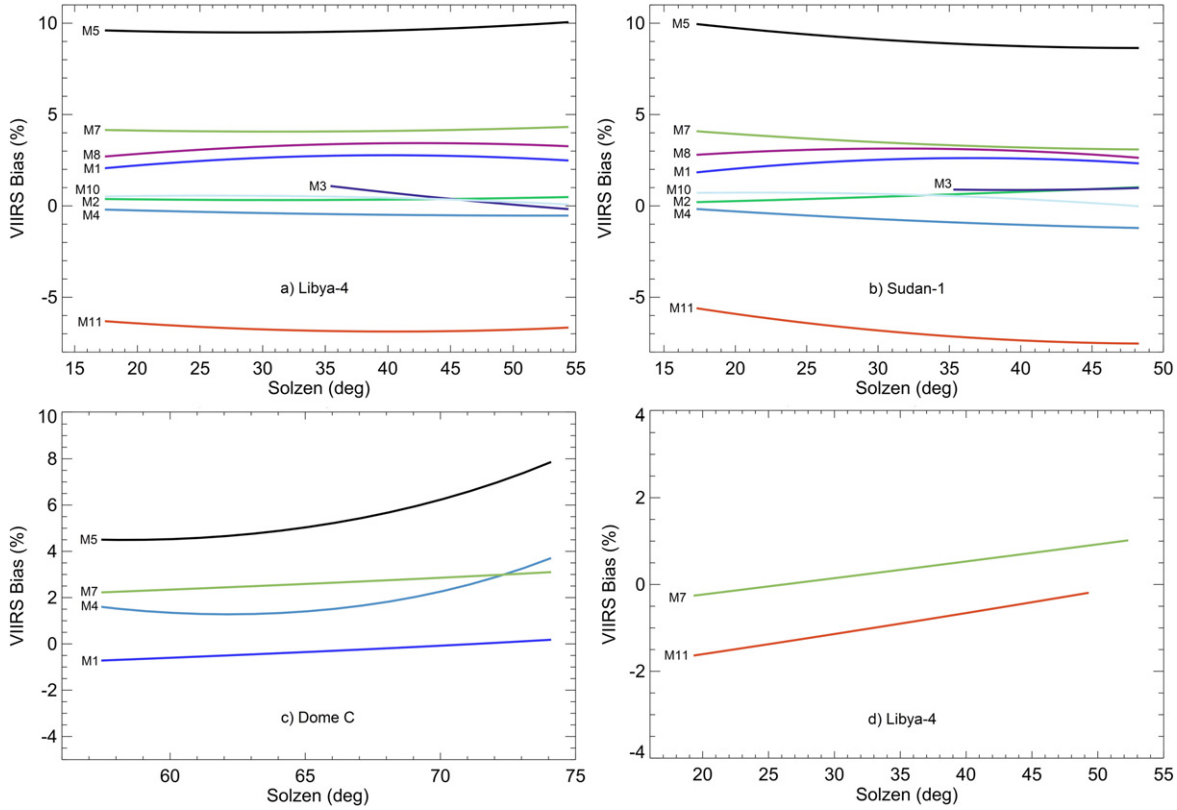

Fig. 5. Bias trends of VIIRS M bands relative to MODIS (figures a, b, c) and relative to OLI (figure d) trends suggest the change in bias as a function of solar zenith angle.

an onboard calibrator with two absolute sources, solar diffuser to calibrate data in reflectance and lamps to calibrate data in radiance. The OLI data in both radiance and reflectance agree very well (2% to 3%) when compared to ground measurements and other well calibrated instruments (Markham et al., 2014; Mishra, Haque, et al., 2014; Mishra, Helder, et al., 2014). Fig. 5d shows the bias trends of VIIRS M7 and M11 over Libya-4 site relative to OLI. Figure indicates that VIIRS and OLI measurements agree well within 2%. Both VIIRS and OLI SWIR bands suggest noisier trends compared to NIR band. M11 has the largest calibration uncertainty.

There are a number of updates in VIIRS calibration parameters since launch that introduced anomalies in the solar diffuser degradation trends (H-factor) and ultimately the gain trends (F factors). It is true that when all data are used in determining the bias, the anomalies in the trend are also attributed to the regression uncertainties. This is one of the reasons we have excluded data during early 2012 when there was a major calibration update on SDSM transmission screen data that affected for more than a month of VIIRS SDR data. After this event, the anomalies in VIIRS calibration have happened few times for short intervals (few days to weeks) that have resulted in changing bias trends over time (trending ups and downs). However the magnitude of bias during these anomalous time periods is still mostly within 2%. Additionally, the numbers of data sets that correspond to anomaly time period are dominated by the normal (no-anomaly) VIIRS calibration data. In addition, this paper analyzes VIIRS data with 16-day repeat cycle based observation. These are the reasons why all data including short term anomalies are included in the bias analysis assuming that the impact on bias uncertainty is small. With the improved calibration and possible reprocessing or the product in future, the uncertainty added due to calibration anomalies can be reduced significantly.

3.3. Spectral analysis of calibration sites

Bias estimated using instrument measurements is dependent on targets utilized in inter-comparison and each target can have different spectral characteristics. If the RSRs of two sensors differ even by a small amount, it may result in bias even when both the sensors are observing the same target with identical viewing conditions. Without accounting for the contributions of RSR mismatch in observed bias, the sensor inter-comparison for quantifying radiometric accuracy is never complete. Calibration sites are analyzed using spaceborne hyperspectral data from EO-1 Hyperion. Fig. 6 shows that Dome C has nearly flat spectra over VNIR region with higher reflectance. Desert sites have higher reflectance towards longer wavelength. Both Dome C and desert sites can be used to quantify impact on observed bias due to spectral differences of sensors. Desert sites have larger reflectance (greater than 60%) for M10 and M11. M8 reflectance spectrum is more flat over desert than Dome C with much higher TOA radiance (on the order of 55 W/[m^2-sr-μm] or more over desert compared to 30 W/[m^2-sr-μm] over Dome C). Thus this study uses only desert sites to evaluate the radiometric performance of VIIRS M8-11.

3.3.1. Spectral band adjustment factors

Spectral band adjustment factor (SBAF) is a term commonly used in inter-comparison to adjust the spectral differences in RSR of the sensors (Chander, Mishra, et al., 2010; Chander, Xiong, et al., 2010; Teillet, Barsi, et al., 2007; Teillet, Fedosejevs, et al., 2007; Teillet, Fedosejevs, & Thome, 2004). SBAF is calculated for VIIRS bands relative to MODIS and OLI using Hyperion data and MODTRAN. It helps to account for the impact of RSR differences in the observed bias such that the residual bias reflects the true biases in the calibration. The resulting VIIRS bias calculated over Libya-4, Sudan-1 and Dome C should agree very well. For VIIRS band M7, the bias computed using MODIS over Libya-4 and using Landsat over Libya-4 need to agree well with each other assuming that the RSR differences are taken into account accurately, and MODIS and OLI bands are accurately calibrated in absolute scale.

Fig. 7 shows SBAF computed over desert and Dome C calibration sites using Hyperion. Since no in-situ measurements are available, this study uses large number of Hyperion observations over the calibration sites to estimate the SBAF. For Libya-4 site, more than 150 Hyperion observations were used to analyze the SBAF. Larger number of Hyperion datasets provides multiple observations over different times of the year with varying atmosphere to make the results more reliable and accurate. Similarly for Sudan-1 site, nearly 90 Hyperion observations were used in the study. Fig. 7 shows that SBAF calculated for VIIRS M11 using VIIRS and MODIS RSR over desert sites is on the order of 7%. The uncertainty is calculated as a one standard deviation of SBAFs. It is interesting to note that M11 has the largest uncertainty of 3.1% over Libya 4 compared to less than 1% over Sudan. The large inconsistency in M11 uncertainty can be due to the fact that VIIRS and MODIS RSR cover different regions of the electromagnetic spectrum which are almost 100 nm apart. The atmospheric variability for these two regions and possible inconsistency in Hyperion bands could be the dominant reasons behind this large spectral bias which needs further investigation. However, VIIRS M11 results in −6.6% SBAF with uncertainty less than 0.5% when compared with OLI matching band. Since OLI completely covers M11 band, the results from VIIRS/OLI can be considered more accurate with lesser uncertainty. Fig. 7 shows that VIIRS M5 (0.67 μm) has the largest SBAF of nearly 7.5% over desert indicating the largest impact on estimated bias (Table 2) due to RSR differences. The rest of the bands have SBAF less than 2% except M10 that suggests nearly 2.5%. Over Dome C, the SBAF for VIIRS M5 is small (2.3%) due to more flat spectra compared to desert. For the rest of the bands, SBAF is on the order of 1% or less. It is to be noted that VIIRS M1 RSR is not covered by Hyperion and hence MODTRAN is used to compute the spectral bias.

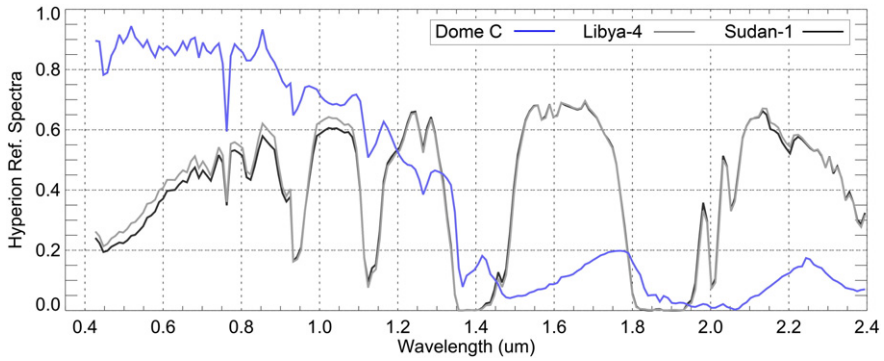

Fig. 6. Spectral characteristics of Libya-4, Sudan-1 and Dome C.

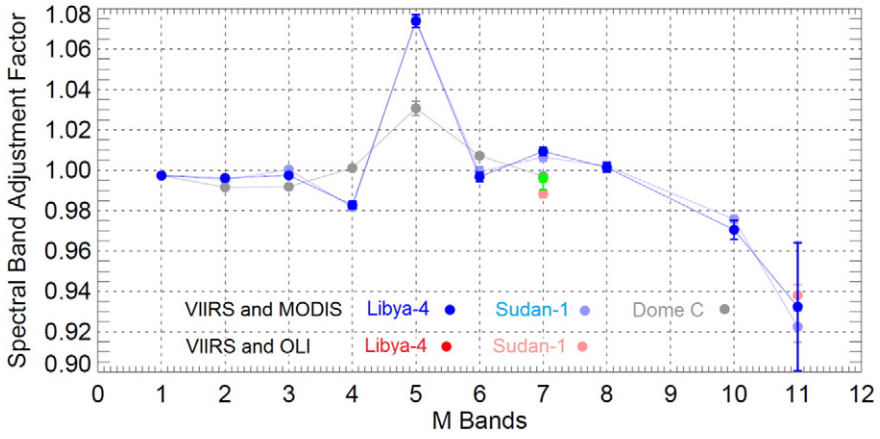

Fig. 7. Spectral band adjustment factors over Libya-4, Sudan-1 and Dome C sites.

3.4. VIIRS radiometric accuracy

When SBAF is accounted for VIIRS observed bias (Table 2), the resulting difference gives the absolute radiometric bias of VIIRS relative to the reference standard (either MODIS or OLI). The uncertainties are mainly contributed from residual BRDF, undetected sub-pixel level cloud contamination, and Hyperion spectral resolution and measurements used to compute SBAF. Fig. 8 shows VIIRS bias for bands M1–11. The VIIRS bias calculated at desert sites and Dome C agree very well to within 1% for bands M2–7 and by 1.5% for M1. M1 SBAF is computed using MODTRAN and couldn't be verified using Hyperion sensor which could be one of the reasons for the larger residual bias. VIIRS bands M1–4 suggest better than 2% ± 1% bias. Similarly for M5, the bias is on the order of 2% over Libya-4 and Dome C whereas it is about 3% over Sudan-1. The root cause could be mainly due to larger mismatch in VIIRS and MODIS RSR. For M7, bias is about 1% when compared to OLI whereas more than 3% when compared to MODIS. This could be due to few reasons; first it could be due to less radiometric accuracy of MODIS; second it could be due to RSR mismatch and third it could be due to SBAF. Hyperion spectral resolution is about 10 nm and it can be observed from spectral characteristics of desert sites in Fig. 8 that there are big changes in Hyperion reflectance around this spectral region. Since VIIRS and MODIS have RSR with wider bandwidth than OLI by about 10 nm in lower wavelength side, the insufficient Hyperion spectral resolution could have resulted in about 2% difference in SBAF between VIIRS/MODIS compared to VIIRS/OLI. This could have possibly been propagated to bias in Fig. 8 where we see discrepancy in residual bias by about 2%. This needs to be further investigated in future. For M8 and M10, the bias is on the order of 3% or more. This might have been caused by calibration inaccuracy in either VIIRS or MODIS. VIIRS M11 suggests 5.4% bias relative to OLI after accounting SBAF. When VIIRS and MODIS are compared for band M11 over Libya-4 and Sudan-1, the estimated radiometric bias is within 2% with uncertainty larger than 3%. Since the spectral coverage of two instruments for this band is about 100 nm apart and the uncertainty is very large, the result doesn't seem to be more reliable as compared to the bias estimated from VIIRS and OLI comparison. The larger uncertainty in M11 could be mainly due to atmospheric absorption variability and the root cause for larger than 5% bias for M11 could be mainly due to inaccuracy in a) VIIRS absolute calibration and b) SBAF estimation.

Table 2
Observed radiometric bias of VIIRS relative to MODIS at desert and Dome C site. Note: Bias is calculated over desert sites at solzen = 18° and over Dome C at solzen = 58° except for a) VIIRS band M2 over Dome C at solzen = 71° and b) M3 over Libya-4 at solzen = 40° and over Dome C at solzen = 78°.

VIIRS		Bias @ solzen = 18°		Bias @ solzen = 58°
Band	Wavelength (μm)	Libya 4	Sudan 1	Dome C
M1	0.402–0.422	1.64% ± 0.35%	1.56% ± 0.46%	−0.14% ± 0.65%
M2	0.436–0.454	0.39% ± 0.31%	0.01% ± 0.46%	−0.50% ± 0.67%
M3	0.478–0.498	0.80% ± 0.24%	1.30% ± 0.32%	−0.20% ± 0.79%
M4	0.545–0.565	−0.16% ± 0.46%	−0.16% ± 0.49%	1.62% ± 1.05%
M5	0.662–0.682	9.6% ± 0.53%	9.92% ± 0.69%	4.86% ± 0.86%
M7	0.846–0.885	4.16 ± 0.72%	4.08% ± 0.88%	2.76% ± 1.35%
M8	1.230–1.250	2.67% ± 1.13%	2.90% ± 1.04%	–
M10	1.580–1.640	0.52% ± 0.64%	0.76% ± 0.64	–
M11	2.225–2.275	−6.38% ± 1.44%	−5.67% ± 1.45%	–

4. Uncertainties

Uncertainties in satellite instrument measurements are mostly dominated by uncertainties in the calibration. VIIRS radiometric stability in this study which is computed using TOA reflectance time series is based on the observations during 16-day satellite repeat cycle. This helps to keep the sensor viewing geometry almost identical throughout the period of study however the change in solar geometry adds BRDF into the data. Analysis of data only at nadir removes the impact of sensor zenith and relative azimuth dependency on BRDF function. The uncertainty in the VIIRS reflectance time series is mostly due to calibration uncertainties, uncertainty in BRDF estimation, atmospheric variability (aerosol, water vapor etc.) and some level of undetected cloud contamination. Instrument stability can be analyzed as a short term vs. the long term. Short term usually refers to time scale of weeks compared to time scale of years in long term stability analysis. Short term stability is dominated by random uncertainty caused by the variability due to limited number of data samples, environmental factors such as clouds and possible calibration updates. Thus the short term stability is generally estimated by using the data variability. In long term, the drift in instrument response over a stable target can be more easily detected in spite of the random uncertainty in the time series. Thus the linear trend in time series over vicarious calibration sites is not recommended to detect the short term stability since a) the uncertainty in the time series can be much larger than the possible drift in the sensor over that period and b) due to the limited observations.

In the inter-comparison between two instruments, uncertainty domain increases further because now we have to deal with the combined uncertainty of two instruments. The data used in the comparison are not usually observed by the two sensors at the same time under the same atmospheric conditions and with identical solar and sensor geometry. A large contribution in uncertainty is from systematic type. Systematic uncertainty in this study mainly comes from a) instrument operational calibration and b) the differences in the spectral response functions of the matching bands under comparison assuming that the target doesn't

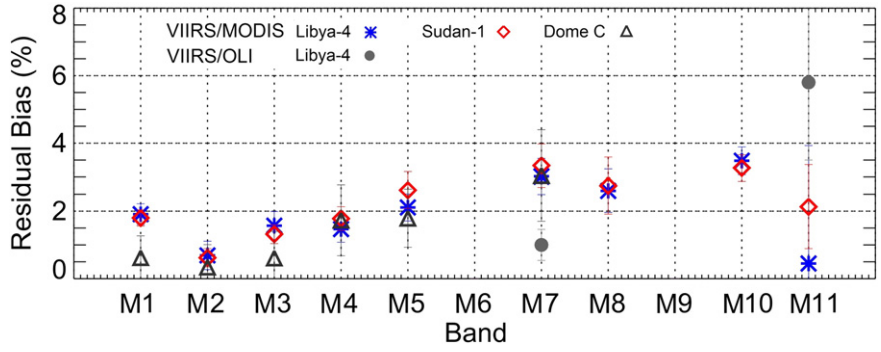

Fig. 8. VIIRS radiometric bias (percent difference between VIIRS and MODIS or OLI), (VIIRS − MODIS) * 100% / MODIS or (VIIRS − OLI) * 100% / OLI.

change. There are no in-situ Hyperion measurements to account for the atmospheric variability. Thus the random uncertainty in SBAF which is mainly due to the uncertainty in Hyperion calibration; possible Hyperion band to band inconsistencies and differences in atmospheric constituents during observation are all embedded into the radiometric accuracy estimation. The largest systematic uncertainty due to RSR differences exists for M11. Since the MODIS and the OLI RSR for matching VIIRS M11 band are near to water vapor absorption spectrum, the uncertainty in radiometric accuracy is even larger. We used MODTRAN to estimate the changes in VIIRS M11 and matching MODIS and OLI reflectance by changing the water vapor contents (from extreme wet with 5.28 g/cm^2 to extreme dry 0.27 g/cm^2 allowed in MODTRAN) for desert target with mid-latitude summer atmosphere. It was observed that the changes were about 3% for VIIRS compared to 10% for MODIS and 9% for OLI. This is one of the reasons that M11 has the largest uncertainty in estimation of SBAF and radiometric accuracy. In this study the VIIRS bias or error is estimated assuming MODIS and OLI as the standard references and uncertainties associated are both random and systematic types.

5. Conclusion

Radiometric performance of VIIRS has been analyzed using well characterized desert calibration sites Libya-4 and Sudan-1. In addition, Antarctica Dome C is also used to quantify the VIIRS performance. The study suggested that VIIRS calibration stability and radiometric accuracy computed at Libya-4 and Sudan-1 sites agree very well. VIIRS moderate resolution reflective solar bands analyzed are temporally stable suggesting no significant trends for most of the bands. M7 indicated to be the least stable band with nearly 1.5% change. Similarly M11 is the noisiest band with the 1-sigma variability of about 1.5%. The calibration uncertainty for the rest of the bands is on the order of 1.0%. VIIRS radiometric bias (analyzed after accounting for spectral differences) relative to MODIS at three sites agrees to mostly within 1%. VIIRS and MODIS agree to within 2% ± 1% for bands M1–4 while M7 and M8 suggest larger bias of nearly 3%. Similarly M5 has bias on the order of 2% at Libya-4 and Dome C however larger than 2% at Sudan-1. VIIRS and OLI intercomparison over Libya-4 suggest 0.9% bias for NIR band M7 and larger than 5% bias for SWIR band M11. The inconsistency in M7 bias of about 2% when compared to MODIS vs. OLI needs to be investigated further. In addition, the larger bias for M11 should be further studied to find out the root cause. The absolute radiometric accuracy calculated for VIIRS is relative to MODIS and OLI. This is the best that can be done at this point due to the limited knowledge about the desert sites. On the other hand, this is the independent validation between the instruments. The study suggests that VIIRS RSB needs to be continuously monitored over well established calibration sites in order to track its on-orbit radiometric performance. This analysis of VIIRS calibration stability and absolute calibration accuracy for RSB will provide an additional source of information which could be useful in improving calibration of the future JPSS/VIIRS instruments. In addition, the results provide understanding on VIIRS SDR accuracy and a path that could help to understand how the impacts could be propagated to EDR products and what the user community can expect in terms of absolute radiometric accuracy, the inter-satellite consistency among EDR products.

Acknowledgements

This work is partially funded by the JPSS program office through grant number NA14OAR4320125. The manuscript contents are solely the opinions of the authors and do not constitute a statement of policy, decision, or position on behalf of NOAA or the U.S. government.

References

Barsi, J.A., Markham, B.L., Helder, D.L., & Chander, G. (2007). *Radiometric calibration status of Landsat-7 and Landsat-5.* Remote Sensing. International Society for Optics and Photonics.

Bhatt, R., Doelling, D., Wu, A., Xiong, X., Scarino, B.R., Haney, C.O., et al. (2014). Initial stability assessment of S-NPP VIIRS reflective solar band calibration using invariant desert and deep convective cloud targets. *Remote Sensing, 6*(4), 2809–2826.

Cao, C., Deluccia, F., Xiong, X., Wolfe, R., & Weng, F. (2013). *Early on-orbit performance of the Visible Infrared Imaging Radiometer Suite onboard the Suomi National Polar-Orbiting Partnership (S-NPP) satellite.* IEEE Trans. Geosci. Remote Sens http://dx.doi.org/10.1109/TGRS.2013.2247768.

Cao, C., Uprety, S., Xiong, J., Wu, A., Jing, P., Smith, D., et al. (2010). Establishing the Antarctic Dome C community reference standard site towards consistent measurements from earth observation satellites. *Canadian Journal of Remote Sensing, 36*(5), 498–513http://dx.doi.org/10.5589/m10-075.

Cao, C., Xiong, J., Blonski, S., Liu, Q., Uprety, S., Shao, X., et al. (2013). Suomi NPP VIIRS sensor data record verification, validation, and long-term performance monitoring. *Journal of Geophysical Research, [Atmospheres], 118*(20), 11,664–11,678.

Chander, G., Mishra, N., Helder, D.L., Aaron, D., Choi, T., Angal, A., et al. (2010). Use of EO-1 hyperion data to calculate spectral band adjustment factors (SBAF) between the L7 ETM+ and terra MODIS sensors. *Geoscience and Remote Sensing Symposium (IGARSS).* IEEE.

Chander, G., Xiong, X., Choi, T., & Angal, A. (2010). Monitoring on-orbit calibration stability of the Terra MODIS and Landsat 7 ETM+ sensors using pseudo-invariant test sites. *Remote Sensing of Environment, 114*, 925–939.

Cosnefroy, H., Leroy, M., & Briottet, X. (2014). Selection and characterization of Saharan and Arabian desert sites for the calibration of optical satellite sensors. Remote Sens. Environ. 1996, 58, 101–114 *Remote Sensing, 6*, 2826.

Folkman, M.A., Pearlman, J., Liao, L.B., & Jarecke, P.J. (2001). EO-1/Hyperion hyperspectral imager design, development, characterization, and calibration. *Proc. SPIE 4151, Hyperspectral Remote Sensing of the Land and Atmosphere* (pp. 40)http://dx.doi.org/10.1117/12.417022.

Helder, D.L., Basnet, B., & Morstad, C.L. (2010). Optimized identification of worldwide radiometric pseudo-invariant calibration sites. *Canadian Journal of Remote Sensing, 36*, 527–539.

Helder, D.L., Markham, B.L., Thome, K.J., Barsi, J.A., Chander, G., & Malla, R. (2008). Updated radiometric calibration for the Landsat-5 Thematic Mapper reflective bands. *IEEE Transactions on Geoscience and Remote Sensing, 46*(10), 3309–3325.

Helder, D.L., Thome, K.J., Mishra, N., Chander, G., Xiong, X., Angal, A., et al. (2013). Absolute radiometric calibration of Landsat using a pseudo invariant calibration site. *IEEE Transactions on Geoscience and Remote Sensing, 51*(3–1), 1360–1369.

Irons, J.R., Dwyer, J.L., & Barsi, J.A. (2012). The next Landsat satellite: The Landsat data continuity mission. *Remote Sensing of Environment, 122*, 11–21.

Knight, E.J., & Kvaran, G. (2014). Landsat-8 operational land imager design, characterization and performance. *Remote Sensing, 6*(11), 10286–10305.

Markham, B., Barsi, J., Kvaran, G., Ong, L., Kaita, E., Biggar, S., et al. (2014). Landsat-8 operational land imager radiometric calibration and stability. *Remote Sensing, 6*(12), 12275–12308.

Markham, B.L., & Helder, D.L. (2012). Forty-year calibrated record of earth-reflected radiance from Landsat: A review. *Remote Sensing of Environment*, *122*, 30–40.

Markham, B.L., Knight, E.J., Canova, B., Donley, E., Kvaran, G., Lee, K., et al. (2012, July). The Landsat data continuity mission Operational Land Imager (OLI) sensor. *Geoscience and Remote Sensing Symposium (IGARSS), 2012 IEEE International* (pp. 6995–6998). IEEE.

Markham, B.L., Thome, K.J., Barsi, J.A., Kaita, E., Helder, D.L., Barker, J.L., et al. (2004). Landsat-7 ETM+ on-orbit reflective-band radiometric stability and absolute calibration. *IEEE Transactions on Geoscience and Remote Sensing*, *42*(12), 2810–2820.

McGuffie, K., & Henderson-Sellers, A. (1985). The diurnal hysteresis of snow albedo. *J. Glaciol*, *31*(108), 188–189.

Mishra, N., Haque, M.O., Leigh, L., Aaron, D., Helder, D., & Markham, B. (2014). Radiometric cross calibration of Landsat 8 Operational Land Imager (OLI) and Landsat 7 Enhanced Thematic Mapper Plus (ETM+). *Remote Sensing*, *6*, 12619–12638.

Mishra, N., Helder, D., Angal, A., Choi, J., & Xiong, X. (2014). Absolute calibration of optical satellite sensors using Libya 4 pseudo invariant calibration site. *Remote Sensing*, *6*, 1327–1346.

Pearlman, J.S., Barry, P.S., Segal, C.C., Shepanski, J., Beiso, D., & Carman, S.L. (2003). Hyperion, a space-based imaging spectrometer. *IEEE Transactions on Geoscience and Remote Sensing*, *41*(6).

Rao, C.R.N., & Chen, J. (1995). Intersatellite calibration linkages for the visible and near-infrared channels of the advanced very high resolution radiometer onboard the NOAA-7,-9, and -11 spacecraft. *International Journal of Remote Sensing*, *16*(11), 1931–1942.

Rao, C.R.N., & Chen, J. (1999). Revised post-launch calibration of the visible and near-infrared channels of the advanced very high resolution radiometer on the NOAA-14 spacecraft. *International Journal of Remote Sensing*, *20*, 3485.

Teillet, P., Barsi, J., Chander, G., & Thome, K. (2007). Prime candidate earth targets for the post-launch radiometric calibration of space-based optical imaging instruments. *Proceedings of SPIE*http://dx.doi.org/10.1117/12.733156.

Teillet, P.M., Fedosejevs, G., & Thome, K.J. (2004). *Spectral band difference effects on radiometric cross-calibration between multiple satellite sensors in the Landsat solar-reflective spectral domain.* Remote Sensing. International Society for Optics and Photonics.

Teillet, P.M., Fedosejevs, G., Thome, K.J., & Barker, J.L. (2007). Impacts of spectral band difference effects on radiometric cross-calibration between satellite sensors in the solar-reflective spectral domain. *Remote Sensing of Environment*, *110*(3), 393–409.

Uprety, S., & Cao, C. (2011). *Using the Dome C site to characterize AVHRR near-infrared channel for consistent radiometric calibration.* SPIE PROC, Earth Observing Systems.

Uprety, S., & Cao, C. (2012). Radiometric and spectral characterization and comparison of the Antarctic Dome C and Sonoran Desert sites for the calibration and validation of visible and near-infrared radiometers. *Journal of Applied Remote Sensing*, *6*(1), 063541.

Uprety, S., Cao, C., Xiong, X., Blonski, S., Wu, A., & Shao, X. (2013). Radiometric intercomparison between Suomi NPP VIIRS and aqua MODIS reflective solar bands using simultaneous nadir overpass in the low latitudes. *Journal of Atmospheric and Oceanic Technology*, *36*, 602–616.

Wang, W., & Cao, C. (2014). DCC radiometric sensitivity to spatial resolution, cluster size, and LWIR calibration bias based on VIIRS observations. *Journal of Atmospheric and Oceanic Technology*, *2014*.

Wu, X. (2004). Operational calibration of solar reflectance channels of the advanced very high resolution radiometer (AVHRR). *Proceedings of SPIE*, *5542*, 272–280.

Wu, A., Cao, C., & Sun, C. (2013). Monitoring NPP VIIRS on-orbit radiometric performance from TOA reflectance time series. *Proc. SPIE 8866, Earth Observing Systems XVIII, 88660Q*http://dx.doi.org/10.1117/12.2023388.

Wu, X., Sullivan, J.T., & Heidinger, A.K. (2011). Operational calibration of the Advanced Very High Resolution Radiometer (AVHRR) visible and near infrared channels. *Canadian Journal of Remote Sensing*, *36*(5), 602–616.

Wu, A., Xiong, X., Cao, C., & Angal, A. (2008). Monitoring MODIS calibration stability of visible and near-IR bands from observed top-of-atmosphere BRDF-normalized reflectances over Libyan Desert and Antarctic surfaces. *Proc. SPIE 7081, Earth Observing Systems XIII, 708113.*

Xiong, X., & Barnes, W. (2006). An overview of MODIS radiometric calibration and characterization. *Advances in Atmospheric Sciences*, *23*(1), 69–79.

Xiong, X., Sun, J., Barnes, W., Salomonson, V., Esposito, J., Erives, H., & Guenther, B. (2007). Multiyear on-orbit calibration and performance of Terra MODIS reflective solar bands. *IEEE Transactions on Geoscience and Remote Sensing*, *45*(4), 879–889.

Xiong, X., Sun, J., & Barnes, W. (2008). Intercomparison of on-orbit calibration consistency between Terra and Aqua MODIS reflective solar bands using the moon. *Geoscience and Remote Sensing Letters, IEEE*, *5*(4), 778–782.

Yamanouchi, T. (1983). Variations of incident solar flux and snow albedo on the solar zenith angle and cloud cover, at Mizuho station, Antarctica. *Journal of the Meteorological Society of Japan*, *61*(6), 879–893.

Yu, F., & Wu, X. (2009). Removal of contaminated pixels from the desert target for AVHRR vicarious calibration. *Journal of Atmospheric and Oceanic Technology*, *26*, 1354–1366.